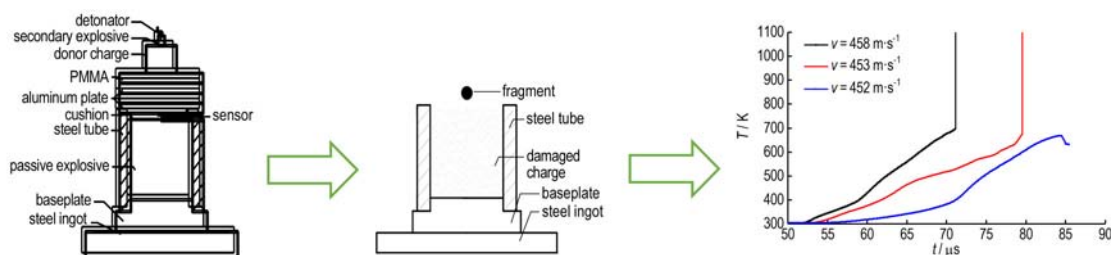


Numerical Simulation on Damaged Charge Ignition by Fragment Impact

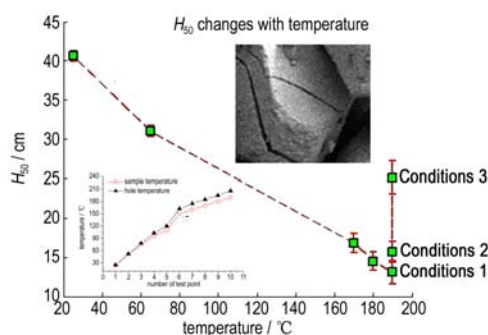


The charge was first damaged by shock waves, and then impacted by fragment. The critical velocities of fragments were obtained. The method of node tie-breaking and the thermo-elastic-plastic model with chemical kinematics equation, describing the ignition of energetic materials, were used in the simulations.

SUN Bao-ping, DUAN Zhuo-ping, LIU Yan, PI Ai-guo, HUANG Feng-lei

Chinese Journal of Energetic Materials, 2019, 27(3): 178–183

Influence Mechanism of Phase Transition and Micro Cracks on Impact Sensitivity of HMX Crystal at High Temperature

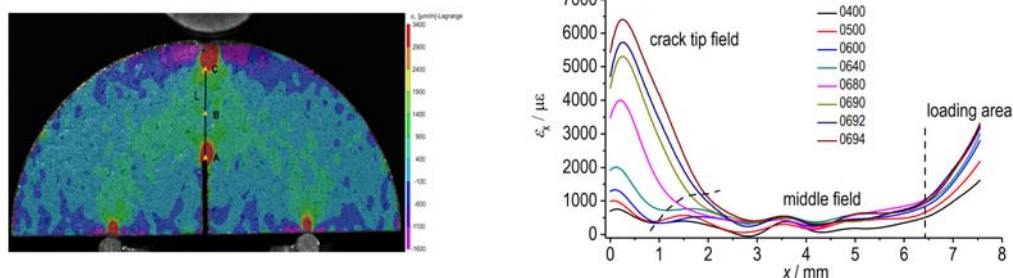


An impact sensitivity testing installation of explosive at high temperature was designed and an impact sensitivity testing method at high temperature was proposed. Combined with the scanning electron microscopy and X-ray diffraction techniques, the impact ignition thresholds of HMX crystal particles to impact process at high temperature were studied by the established test method.

WEN Yu-shi, WEN Wen, DAI Xiao-gan, WEN Mao-ping, LONG Xin-ping, ZHENG Xue, YAO Kui-guang, HE Song-wei, LI Ming

Chinese Journal of Energetic Materials, 2019, 27(3): 184–189

Opening Mode Crack Initiation and Propagation Behavior of TATB-based PBX

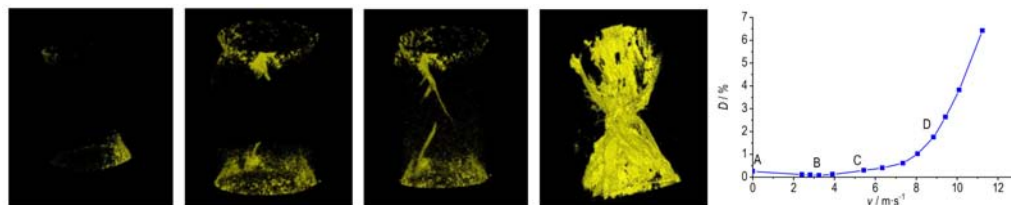


A semi-circular bending specimen with pre-fabricated crack was designed to study the initiation and propagation behavior of crack for TATB-based PBX, the principle strain distribution and evolution characteristic at crack tip field and crack path were obtained using digital image correlation method.

LIU Chen, LAN Lin-gang, CHEN Hua, TANG Ming-feng, GAN Hai-xiao, LI Ming

Chinese Journal of Energetic Materials, 2019, 27(3): 190–195

Impact Damage Characteristics of TATB-based Polymer Bonded Explosive Under Confining Pressure Based on the CT Image Sequences

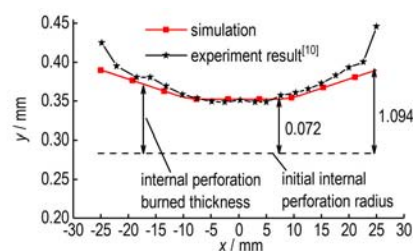
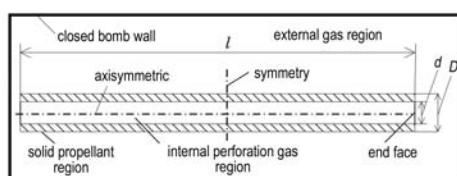


The separated Hopkins pressure bar was used to impact the PBX and the damage was observed by X-ray micro-computed tomography(X- μ CT). Based on CT image sequences and combined with digital image processing algorithm, the extraction and 3D reconstruction of damaged cracks was performed. A damage variable evaluation method based on the proportion of defect volume in CT images was proposed to calculate and analyze the value of damage variable under different impact velocities of bullet.

LIU Ben-de, CHEN Hua, ZHANG Wei-bin, ZHANG Cai-xin,
LIU Chen

Chinese Journal of Energetic Materials, 2019, 27(3):196–201

Internal Perforation Erosive Burning and Flow Characteristics of Tubular Propellant

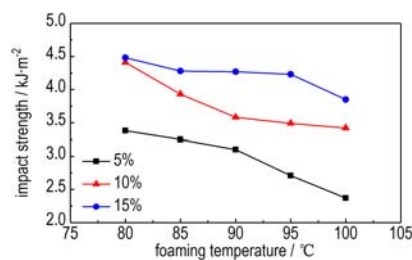
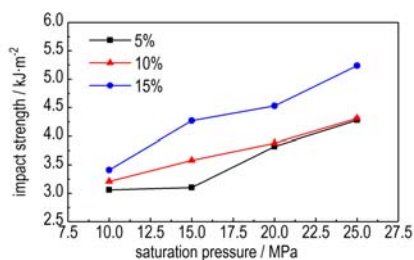


A single perforation stick propellant closed bomb model was established to study the internal perforation erosive burning and flow filed. The closed bomb is divided into three regions: the external gas region, solid propellant region and internal gas region. It's a useful approach to reveal the erosive burning process in the combustion process.

ZHAO Xiao-liang, ZHANG Xiao-bing

Chinese Journal of Energetic Materials, 2019, 27(3):202–209

Fabrication and Mechanical Properties of Micro-porous NCTEGN/RDX Composites

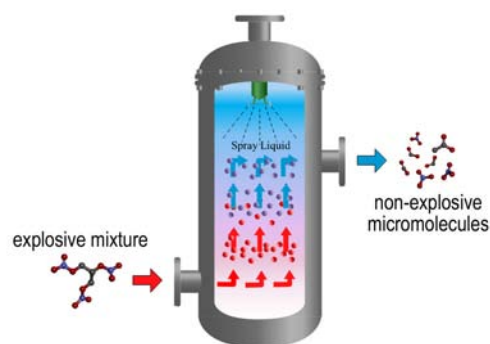


Micro-porous combustible composites of NC / TEGN / RDX were fabricated by supercritical carbon dioxide foaming process. The effect of saturation pressure and foaming temperature on the internal structure and mechanical properties of the composites was investigated.

ZHANG Shuo, DING Ya-jun, YING San-jiu

Chinese Journal of Energetic Materials, 2019, 27(3):210–215

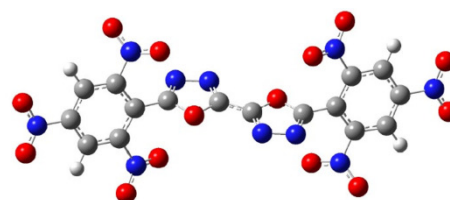
Explosion-elimination of Gaseous Nitrolycerin During the Production Process of Tri-base Gun Propellant



LIU Bing-xin, HAN Kun-xiang, SUN Zhi-yang, CHEN Peng-peng,
ZHANG Zhi-fang, LIU Da-bin, QIAN Hua
Chinese Journal of Energetic Materials, 2019, 27(3): 216–219

Explosive mixture can be eliminated and decomposed into non-explosive micro molecules by alkaline solution, in this case, the organic solvent, such as ethanol and acetone, can be recovered safely.

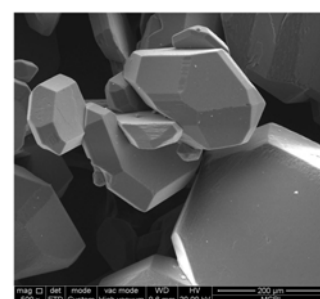
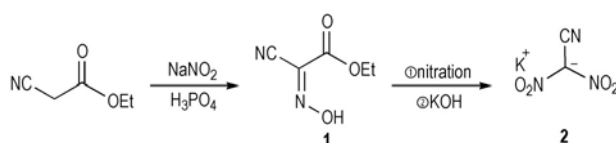
Synthesis Optimization and Properties of TKX-55



LIU Yang, SHEN Cheng, LU Ming
Chinese Journal of Energetic Materials, 2019, 27(3): 220–224

5, 5'-Bis(2, 4, 6-trinitrophenyl)-2, 2'-bi(1, 3, 4-oxadiazole) (TKX-55) was synthesized from trinitrotoluene. The optimal chlorination and substitution reaction conditions were obtained. The chemical structure of TKX-55 was characterized by infrared (IR) spectroscopy, nuclear magnetic resonance (NMR). The detonation velocity and detonation pressure are calculated by Kamlet-Jacob formula.

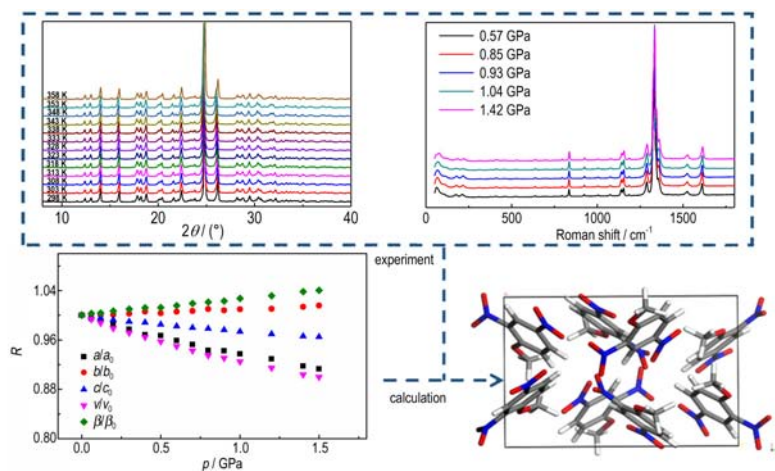
Synthesis, Thermal Behavior and Crystal Morphology of Potassium Dinitroacetonitrile



LI Xiang-zhi, BI Fu-qiang, ZHOU Cheng, ZHOU Qun,
WANG Bo-zhou
Chinese Journal of Energetic Materials, 2019, 27(3): 225–229

Potassium dinitroacetonitrile was synthesized via the reactions of nitrosation, nitration-hydrolysis. The samples of potassium dinitroacetonitrile with different crystal morphology were prepared by adding the different surfactants, changing the cooling rate and stirring speed. The thermal decomposition process of potassium dinitroacetonitrile with different crystal morphologies was studied by DSC, and their mechanical sensitivities were tested.

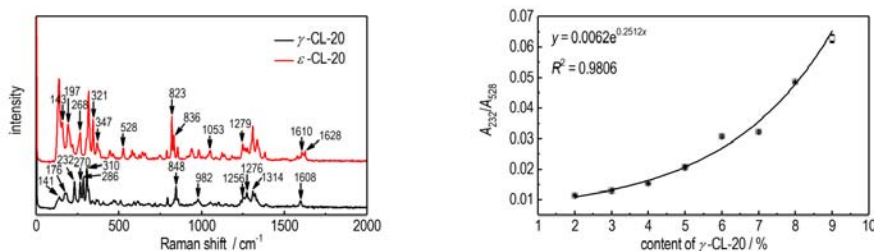
Crystal Structure and Mechanical Properties of α -DNAN Under Temperature-Pressure Coupling



2,4-Dinitroanisole (α -DNAN) might be a potential candidate for the slow component of plane wave lens. The phase transition, densities and mechanical properties of α -DNAN under variable temperatures and pressures were studied by theoretical and experimental methods.

LI Hua-rong, YANG Yong-lin, ZONG He-hou, YU Hai-jiang
Chinese Journal of Energetic Materials, 2019, 27(3): 230–235

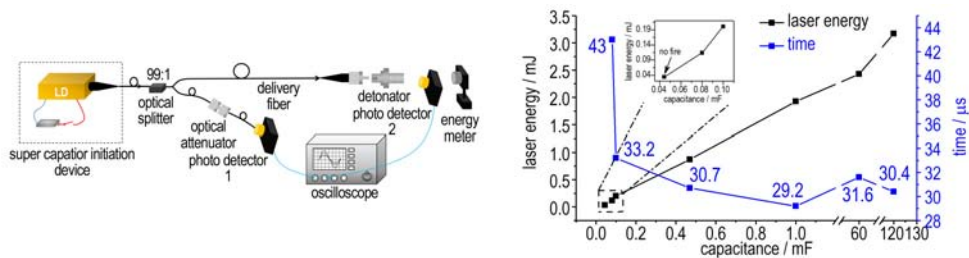
Analyzing Crystal Form Purity of Hexanitrohexaazaisowurtzitan (CL-20) by Raman Spectroscopy



A rapid and sensitive quantitative method via Raman spectroscopy was explored for the measurement of crystal purity of ϵ -CL-20.

GAO Feng, MENG Zi-hui, LIU Wen-fang, LI Zhi-xue, WANG Ming-hui
Chinese Journal of Energetic Materials, 2019, 27(3): 236–241

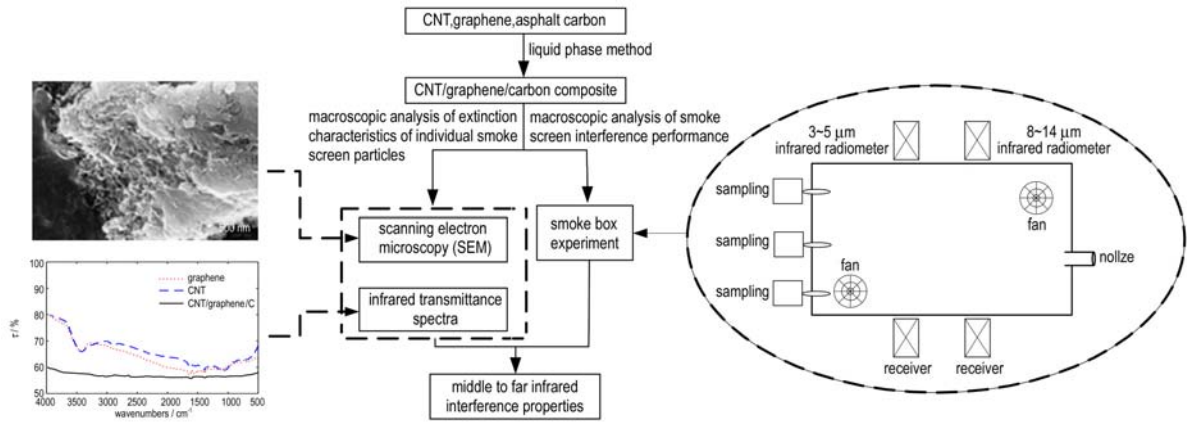
Laser Initiation BNCP Driven by Super Capacitor



The rule of laser detonates driven by super capacitor were investigated using seven different capacitance values and five different discharge voltages. The study reveals that the driving method of laser diode driven by super capacitor can significantly shorten the laser initiation delay.

WANG Hao-yu, CHU En-yi, HONG Jin, HE Ai-feng, CAO Chun-qiang, JING Bo, MA Yue, HU Ya-dong
Chinese Journal of Energetic Materials, 2019, 27(3): 242–248

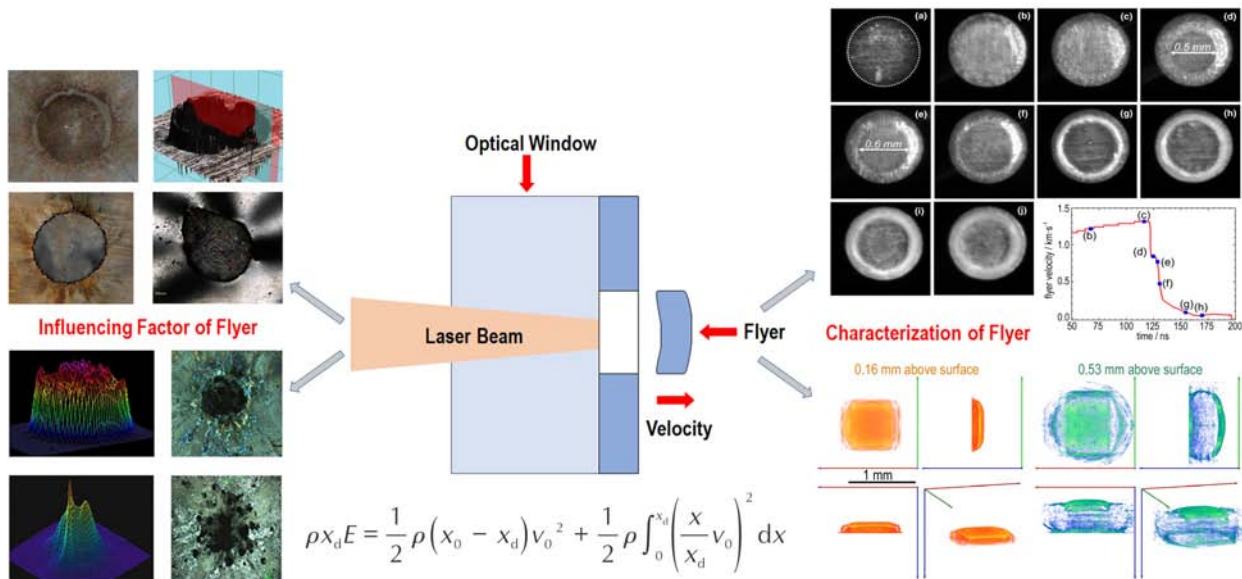
Middle and Far Infrared Interference Properties of CNT/Graphene/Carbon Composites Smoke Screen



The carbon nanotube/graphene/carbon composites were prepared by liquid phase method. The microstructure and infrared absorption of graphene, carbon nanotubes and composites were compared by scanning electron microscopy and infrared spectroscopy. Based on the smoke box experiment, the interference performance of graphene, carbon nanotubes and composite materials to middle and far infrared was analyzed.

CHEN Hao, GAO Xin-bao, XU Xing-chun, ZHANG Qian, ZHANG Kai-chuang
Chinese Journal of Energetic Materials, 2019, 27(3): 249–254

Research Progress in the Flight Characteristics of Laser-driven Flyer



The research progress of laser-driven flyer was briefly reviewed. The methods characterizing the flying process of laser-driven flyer were introduced. Thus, the current unclear influencing factors on flight properties of laser-driven flyer is the focal points of laser-driven flyer which need further and deep studies.

WANG Zhi-hao, LI Yong, QIN Wen-zhi, GAO Yuan, JIANG Xiao-hua, WANG Liang, HE Bi
Chinese Journal of Energetic Materials, 2019, 27(3): 255–264

Executive editor: WANG Yan-xiu GAO Yi ZHANG Qi JIANG Mei